J. Agr. Sci. Tech. (2022) Vol. 24(2): 365-378

Modeling Honey Adulteration by Processing Microscopic Images Using Artificial Intelligence Methods

M. Pirmoradi[1], M. Mostafaei[1*], L. Naderloo[1], and H. Javadikia[1]

ABSTRACT

The aim of this study was to determine the authenticity of honey by processing microscopic images and obtaining an algorithm for classifying various honey frauds. In this study, sucrose, fructose, and fructose-glucose solution at a ratio of 0.9 were used to make honey adulteration. The level of adulterated honey was based on the weight percentages of 2.5, 5, 7.5, 10, 20, 30, 40, 50, 60, 70, 80, 90 and 100 by stirring. Different samples were imaged under a microscope. Each image was processed in 33 monochrome color spaces and 15 parameters were extracted from it. The three main and effective parameters of various color spaces were selected using sensitivity analysis for modeling honey fraud by adaptive Fuzzy Neural Inference System (ANFIS), Artificial Neural Network (ANN), and response surface methodology. Various criteria were used to evaluate the performance of the models such as coefficient of determination, mean square error, sum of squared estimate of errors, and mean absolute errors. The results showed that the determination coefficient and the mean square error of the artificial neural network model was 0.974 and 0.0024, respectively. Finally, using the desirability function, the artificial neural network model was selected as the best model due to less prediction error values and desirability of 0.948.

Keywords: Adaptive fuzzy neural inference system, Artificial neural network, Desirability function, Response surface methodology.

INTRODUCTION

Honey is a sweet natural food substance produced by bees. Honeybees collect and transport the nectar of blossoms, secretions of living parts of plants, or excretions of plant-sucking insects. Then, they combine it with their own particular body materials and store them in the hive until the process is over (Standard, 2001).

Typically, honey adulteration can be direct or indirect. Today, with the increasing production of fermented and natural syrups, their direct addition to honey is a widespread form of adulteration. For example, honey adulteration was reported by mixing it with fructose syrup (Li *et al.*, 2012). The honey adulteration with High Fructose Corn Syrup (HFCS), Glucose Syrup (GS) and Sucrose Syrup (SS) can be detected by isotope ratio mass spectroscopy. Honey adulteration by adding C4 plant sugar (GS-HFCS) was detected by this method while adulteration by C3 (SS) was not detected (Tosun, 2013). Previous studies have shown that expensive, highly specialized, and time-consuming methods and tools are required to determine the extent of adulteration in honey. In this context, various methods including spectroscopy, chromatography, differential scanning calorimetry, electronic instruments and sensors, or the combination of these methods can be used (Agila, and Barringer, 2013; Anthony and Balasuriya 2016; Cordella *et al.* 2003; Du *et al.* 2015; Zakaria *et al.* 2011; Salvador *et al.* 2019).

The high capability (speed, low cost) of image processing methods in the food industry has been known for a long time.

[1] Department of Mechanics of Biosystems Engineering, Razi University, Kermanshah, Islamic Republic of Iran.
[*] Corresponding author; e-mail: b.mostafaei@razi.ac.ir

Food industry is one of the first ten pioneer industries that has benefited from image processing methods as this method has succeed in offering a non-destructive evaluation approach for the food products (Du and Sun 2004).

Various methods have been reported in the literature, including chromatographic methods, UV-Vis spectroscopy, vibrational spectroscopy, hyperspectral imaging, differential scanning calorimetry, dielectric spectroscopy, and nuclear magnetic resonance spectroscopy with linear discriminant analysis to describe and classify food products, as well as to detect and quantify food contaminants (Esteki *et al.* 2017; Esteki, Simal-Gandara, *et al.* 2018; Esteki, Shahsavari, *et al.* 2018; Yang *et al.* 2018; Fahim Danesh and Bahrami 2015; Khorsandmanesh *et al.* 2020).

A study addressed the use of classification-based hyper-spectral imaging and data mining systems to detect honey adulteration. Hyper-spectral images (400-1,000 nm) were captured from pure and adulterated samples using Vis-NIR spectroscopy. The results of the classification tests showed the highest classification accuracy of 95% for the Artificial Neural Network (ANN) method (Shafiee, *et al.* 2016).

In a microscopic study on the honey, a laboratory method was employed to separate and detect sunflower pollen. This method was based on ARGUS image processing to reduce the pollen analysis and origin determination time (Cseke, *et al.* 1993). In the mentioned study, the author expressed that the pollen quantity of each slide will determine adulteration in honey.

To investigate the sucrose syrup adulteration in honey, microscopic analysis can also display parenchyma cells, single-arterial vessels, and epidermal cells. Generally, due to low technology and high impurities in the production of syrups, microscopic methods can screen the product to detect the fraud of sugar cane products in honey (Kerkvliet *et al.* 1995). Honey adulteration is expanding. Various types of honey fraud exist; but no method has been developed for the simultaneous detection of all these adulteration (DU *et al.* 2015).

In this research, various types of syrups such as sucrose, fructose and fructose-glucose solution at the ratio of 0.9 were used at different levels to create honey adulteration. Adaptive Neuro Fuzzy Inference System (ANFIS), ANN, and Response Surface Methodology (RSM) approaches were also employed to model and determine the amount of adulteration. The performance of models was evaluated by statistical criteria such as R^2 (Coefficient of Determination), MSE (Mean Squared Error), SSE (Sum of Squared estimate of Errors), and MAE (Mean Absolute Error). The aim of this study was to find an algorithm for determining the honey authenticity by differentiating the amount of pollen and insoluble solids in microscopic images regardless of the type of adulteration (nutritional or additive) and the type of the applied syrup.

MATERIALS AND METHODS

The fennel honey was obtained from the beekeepers at Kangavar Area of Kermanshah, Iran. In order to ensure that the honey was not adulterated, three hives were randomly selected from this area. To have natural and highly pure honey, the beekeepers were asked not to give any nutritional syrup to these hives.

Pollen Analysis (Melissopalynology) to Prove the Type of Feeding Flower

The honey extracted from the hives was investigated to determine the source of the plant (fennel) by pollen analysis method, prior to the research process. For this purpose, 20 g of pure honey samples were dissolved in 40 mL distilled water at 30°C. The specimens were then centrifuged at 3,000 rpm for 15 minutes using a Rotina 46 R centrifuge (Het-Tich

Zentrifugen, Germany). The upper phase was removed and sediment mixed with 10 mL solution of sulfuric acid (Merck, Germany) and acetic acid (Merck, Germany) at the ratio of 1:9, it was then placed in a bain-marie (or water bath) at 60°C for 10 minutes (acetolysis). The samples were centrifuged at 3,000 rpm again and the supernatant was removed. The sediment mixture was then dispersed on a glass slide. Each analysis was performed in 3 replications. At least 500 pollen grains were counted for confirmation of the botanical origin (Anjos *et al.*, 2015). More than 46% of the pollen, as shown in Figure 1-a, was depicted in the image of fennel pollen, which corresponded to Figure 1-b derived from the scientific sources of pollenology (D'Ávila, *et al.*, 2016).

Sample Preparation and Imaging

The microscope chosen for the sample capture was a Dino-Lite Edge AM4515ZT. This device provides a resolution of 1280×1024 pixels images (Figure 2-a). In this study, three syrups were used to make adulteration: sucrose, fructose and fructose-glucose solution with ratio of 0.9, which is close to the natural composition of honey. To prepare 100 g of sucrose syrup, 66.62 g of pure sugar of commercial grade was dissolved in 33.28 g of deionized water at 20°C with weight ratio of 2:1 (Asadi, 2006). The treatments of triple syrups were mixed with honey at percentage levels of 0, 2.5, 7.5, 10, 20, 30, 40, 50, 60, 70, 80, 90 and 100 (weight) by agitator for 3 minutes, and then kept in bain-marie at 35°C for 20 minutes in order to homogenize (Bidin, *et al.*, 2016). Then, 20 g of samples were dissolved in 40 mL distilled water at 30°C without using the acid, the samples were then centrifuged at 1,500 rpm for 10 minutes. The upper phase was separated and distilled water added to sediment for the second time and centrifuged at 1,500 rpm once again. Finally, 5 µL of sediment mixture was placed on a Lam. The glass slide of samples was prepared by placing the Lamel on the Lame, for uniform spreading

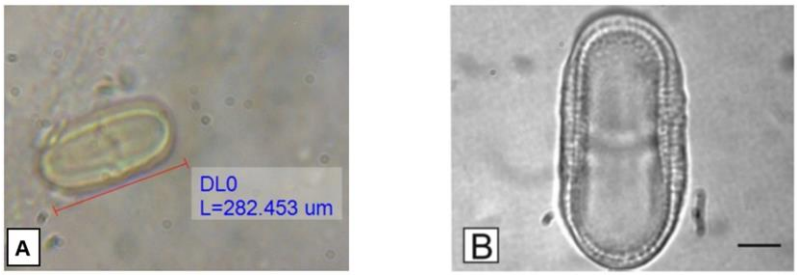

Figure 1. (a) Image of fennel pollen in this research, and (b) Equator view of fennel pollen from scientific sources.

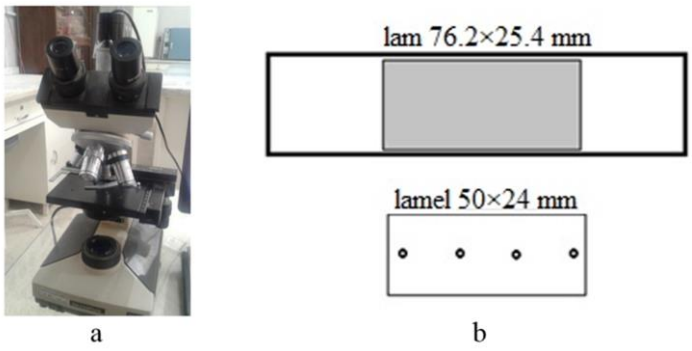

Figure 2. (a) Image capturing devise, and (b) Schematic of glass slide (Lamel and Lam).

of materials (Figure 2-b). For uniform imaging, four points were determined on the symmetry line of the Lamel. The difference between pollen and other insoluble solids was evident in microscopic images (Figure 3). The dispersion of the sediment is oval and decreasing trend from the center of the Lamel to the sides. Therefore, each slide photo could be full or empty from pollen and insoluble solids, but the average value of the parameters examined in all photos in each sample was in relation to the amount of adulteration.

Image Processing

In this study, in order to have more features in the process of image processing, color space for RGB (Red, Green, and Blue channels), CMY (Cyan, Magenta, and Yellow channels), BW (Black and White channels), HSV (Hue, Saturation, and Value channels), $I_1I_2I_3$ (linear relationship of the components of this space with the RGB space), Lab (a pixels light converted into the L channel with a and b color channels), NrNgNb (normalized RGB values), YCbCr [converted of an RGB image to luminance (Y), and Chrominance (Cb and Cr) values], YCrCgCb (the brightness information from the conversion of RGB space by a Y component), YIQ [luminance (Y) and chrominance information], YUV [luminance (Y) and two color difference (U, V) components] and Gray channels of MATLAB Image Processing Toolbox were used. Other types of color spaces could be obtained using linear or nonlinear transfer functions (Gonzalez and Woods 2002). Also, classification systems such as ANFIS, ANN and RSM were employed by MATLAB 2013b and Design Expert 10 software, respectively.

Evaluating Model Performance

For evaluating the performance of the obtained models, different statistical criteria were used such as coefficient of determination, mean square error, sum of squares for error and mean absolute error. Equations (1) to (4) shows these criteria (Mostafaei, 2018).

$$R^2 = 1 - \frac{\sum_{S=1}^{n}(X_S - X_0)^2}{\sum_{S=1}^{n}(X_S - X_m)^2} \quad (1)$$

$$\mathrm{MSE} = \frac{1}{n}\sum_{S=1}^{n}(X_S - X_0)^2 \quad (2)$$

$$\mathrm{SSE} = \frac{1}{n}\sum_{S=1}^{n}(X_S - S_m)^2 \quad (3)$$

$$\mathrm{MAE} = \frac{\sum_{S=1}^{n}|(X_S - X_0)|}{n} \quad (4)$$

In these equations, X_S is the actual values, X_0 is the predicted values, X_m is the average of actual values, S_m is the average of predicted values and n is the number of predicted values.

The four different statistical indicators may be different, and the model is not

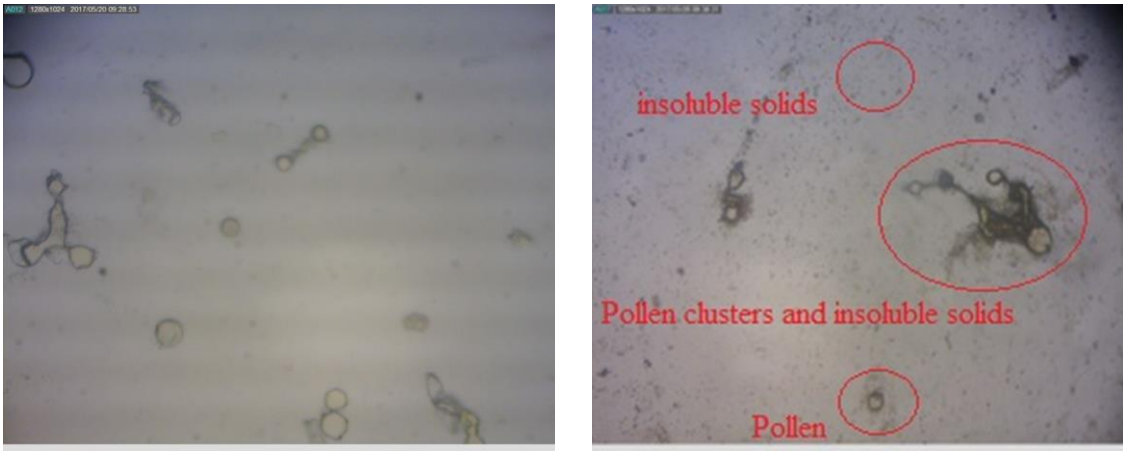

Figure 3. Microscopic images, pollen and solids in the sediment.

optimal at the same time for all indicators; therefore, by defining the desirability function as Equations (5) to (7), the optimal model was introduced for predicting the adulteration (Myers *et al.*, 2016). Of course, it should be noted that the weight and importance of each index were assumed the same. If the response (y) is maximized, its partial desirability is defined as follow:

$$d_i = \frac{y-L}{U-L} \quad (5)$$

The minimal desirability of the response (y) is defined below:

$$d_i = \frac{U-y}{U-L} \quad (6)$$

The total desirability function for each model is defined in Equation (7):

$$D = (d_1 \times d_2 \times ... \times d_n)^{1/n} \quad (7)$$

In these equations, d_i, y, L, U, D and n are partial desirability of each response, value of response (relevant index), smallest amount of response, maximum amount of response, total desirability function, and the number of responses, respectively.

RESULTS AND DISCUSSION

In general, each of the images taken from the honey samples were examined in 33 single color channels, including a channel of Gray, two channels of BW, and three channels for each of the 10 color spaces mentioned above. In each monochrome channel, 15 parameters were measured: minimum, mean, maximum, standard deviation, mode, correlation coefficient, variation range, skidding, stretching, entropy, variance, median, harmonic average, covariance and contrast. In other words, 33×15 parameters or 495 inputs were extracted from each image for modeling process. Due to the difference in the amount of components in the microscopic slide, an algorithm was developed for the separation of honey based on the amount of adulteration. According to the mentioned pollen analysis method in the sampling section, six replicates (slides) were prepared from each treatment. In each slide, four distinct image points were recorded; therefore, for each type of fraud, 24 images were captured in each treatment and 984 images were taken at all 41 treatments. As mentioned above, 495 parameters were processed from each image and, therefore, 11,880 image parameters were processed for each treatment. For modeling process, the average of all of the parameters obtained from 24 images of each treatment were examined.

Some color channels are shown in Figure 4. As it is known, the HSV, BW, $I_1I_2I_3$, Lab, NrNgNb, YCrCgCb channels do not provide a specific resolution of the image components, unlike the RGB, YCbCr, YIQ, Gray, YUV and CMY channels. In the YIQ channel, the highest resolution of the image components (pollen clusters and insoluble solids) is more clearly specified.

Sensitivity Analysis

Using all of the parameters obtained from the images will cause the models to be in error and inefficient. Therefore, using sensitivity analysis, the parameters were identified that were more sensitive to the amount of fraud. It was tried to select channels and monochrome images of each channel that seemed appropriate and had a good separation of color (Figure 4). Then, by limiting some of the features, the sensitivity analysis was used to select the best inputs of the models. According to the importance of sensitivity analysis, the selected inputs included the minimum value of R for RGB images, the minimum G value for RGB images, the minimum B value for RGB images, the minimum Y value for YCbCr images, the minimum Y for YIQ images, the minimum value for Gray images, the minimum Y value for YUV images and the maximum Y value for CMY images. The results obtained from the sensitivity analysis of the eight inputs are shown in Figure 5. The rest of the parameters had a much lower sensitivity to the amount of fraud. According to Figure 5, the minimum Y of single-color image is shown as the most sensitive parameter in the YIQ color channel. Therefore, the three selected input parameters for modeling were the minimum R value for RGB images, the

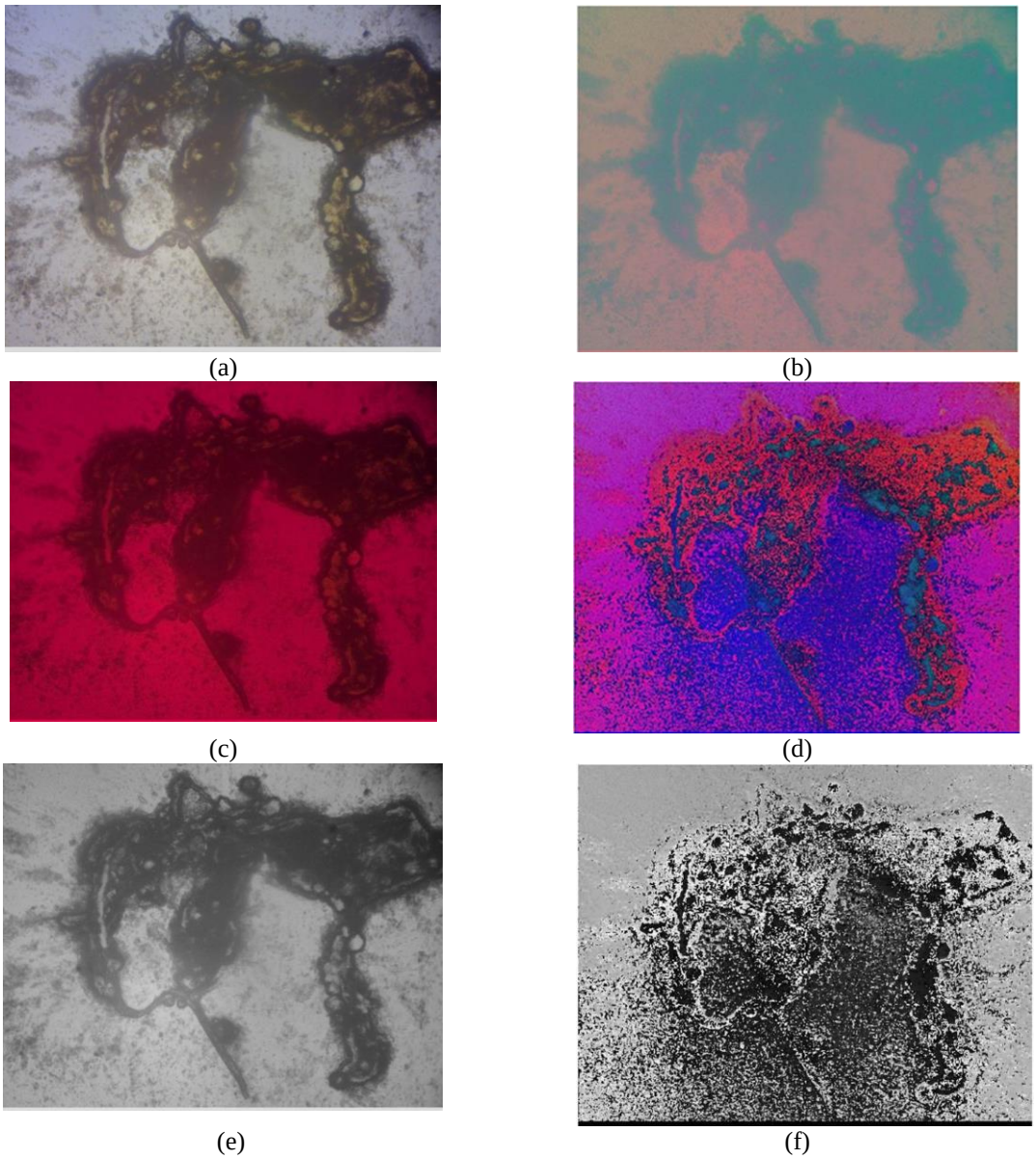

Figure 4. Display of color channels for pollen clusters and insoluble solids: (a) Original image (RGB), (b) YCbCr, (c) YIQ, (d) HSV, (e) Y of color channel (YIQ), and (f) H of color channel (HSV).

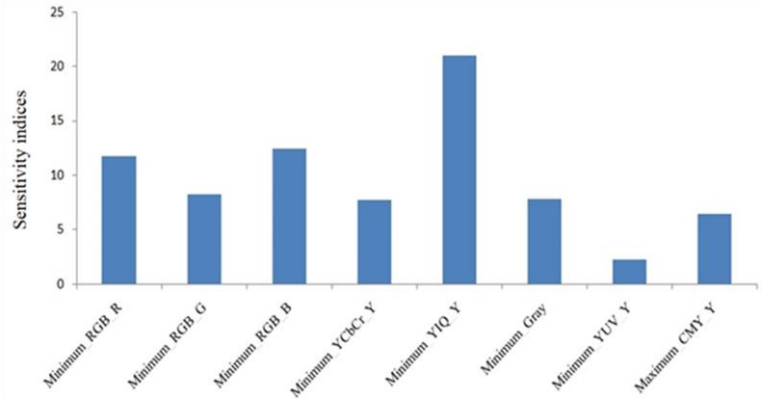

Figure 5. Sensitivity analysis of the eight selected parameters relative to the percentage of honey adulteration.

minimum value B for RGB images, and the minimum Y value for YIQ images.

Modeling the Percentage of Honey Adulteration Using ANFIS Approach

For ANFIS approach, the three mentioned parameters in sensitivity analysis i.e. the minimum R value for RGB images, the minimum value B for RGB images, and the minimum Y value for YIQ image were used as input variables and the amount of honey adulteration was used as output of the model. To begin the model development process, the collected data was randomly divided into two data sets: training (70% of all data) and test (30% of all data). The structure of the best ANFIS model and the performance parameters of the model for predicting honey adulteration are shown in Tables 1 and 2, respectively.

The correlation and fitting of the experimental and predicted adulteration for the test and all data set are shown in Figure 6. In this figure, the large (green color) and small (red color) scatter graphs were found for all data and test data, respectively. As shown in this figure, there is good fitness between actual adulteration and predicted value by the ANFIS model. The value of the determination coefficient (R^2= 0. 973) indicates that only 2.74% of the total variations cannot be explained by this model. The dispersion of data around the regression of the model (error) was in an acceptable situation.

Modeling the Percentage of Honey Adulteration Using ANN Approach

For ANN approach, the multi-layer perceptron network or the feed forward neural network was used. The input parameters of the neural network model were the same three high sensitive parameters obtained from the analysis of sensitivity and output of the model was also amount of adulteration. Also, 30% of the data was used for testing and the rest for training. The best neural network structure for detecting the amount of fraud is presented in Figure 7. This model was selected using trial and error algorithm from dozens of different models with different structures. The characteristics of this model and its functional parameters are presented in Tables 3 and 4, respectively. As shown in Figure 7, the selected model has three inputs, two hidden layers with four and one neuron, and Tansig transfer function. In the output layer, according to the number of outputs of the model, only one neuron has a linear transfer function. Among the different methods of training in the method of back propagation of errors, the Levenberg-Marquardt algorithm was selected for use in the present study due to faster convergence in the training of medium-sized networks.

Table 1. Characteristics of the best ANFIS model to estimate the honey adulteration.

Number of input	Number of Membership Function (MF) for each input	MF type	Output type	Optimization method	Number of epoch
3	3	triangular	Linear	grid partition	100

Table 2. The performance parameters of the best ANFIS model to estimate the honey adulteration.

	No of data	MSE	MAE	SSE	R^2
Training	29	0.0026	0.0290	0.0750	0.9793
Test	12	0.0046	0.0482	0.0550	0.9549
All data	41	0.0032	0.0346	0.1301	0.9726

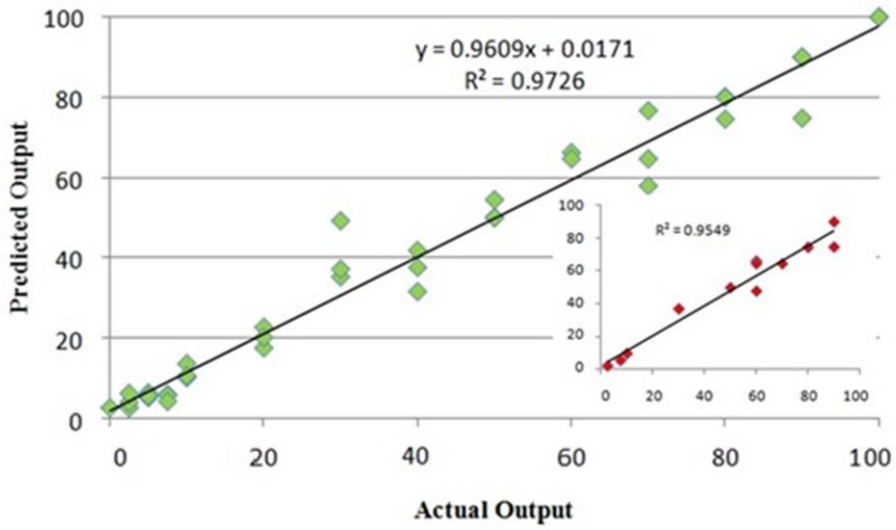

Figure 6. Correlation between actual data of honey adulteration (%) and predicted ones by ANFIS model.

The fitting graphs of actual and predicted data for all data and test data are shown in Figure 8. As is clear from the form and the coefficient of determination, the ANN model fitted better than the ANFIS model. Also, the greatest advantage of this model was the less error and the smaller difference between the predicted value and the actual value of the regression line.

The BP-ANN neural network model was previously used for detecting adulteration by combining d-fructose and d-glucose syrups with an original mass ratio of honey at levels of 5%, 10%, 15% and 20% to honey using visible absorption spectroscopy and ultraviolet light was combined with a chemo-metrics. This study showed that UV-Vis absorption spectroscopy based on PCA and BP-ANN could be used as a suitable, fast, and accurate technique to identify valid counterfeit honey (Ou *et al.*, 2011). In the past, back propagation neural network was used to determine the level (1 to 25%, w/w) of invert sugar cane sugar in honey by the FT- IR ATR with a predictive success rate of 93.55% (Irudayaraj, *et al.* 2003). To identify the rice syrup fraud in honey, it was found that BP-ANN was the most appropriate model. This showed that the BP-ANN model could be fast, non-destructive, and accurate in identifying adulteration of honey (Chen, *et al.*, 2014; Ouyang, 2013). In another study, it was exhibited that use of the hyper-spectral imaging and data mining system based on the ANN classification had the highest accuracy rating of 95% for detecting honey adulteration (Shafiee, *et al.* 2016).

Modeling the Percentage of Honey Adulteration Using RSM

The Design Expert software was used for modeling the percentage of honey adulteration by historical data design. The best obtained model was fitted to a third-order polynomial equation (Cubic). The functional parameters of this model are presented in Table 5 and the regression graph of test and all data are presented in Figure 9. Comparison of ANN, ANFIS and RSM models showed that in training, test, and all data in RSM model the error (difference between predictive values and actual value) was highest (MSE= 0.0115) and the determination coefficient of this model was lowest (R^2= 0.873). Therefore, the efficiency and accuracy of the response surface model to predict the honey

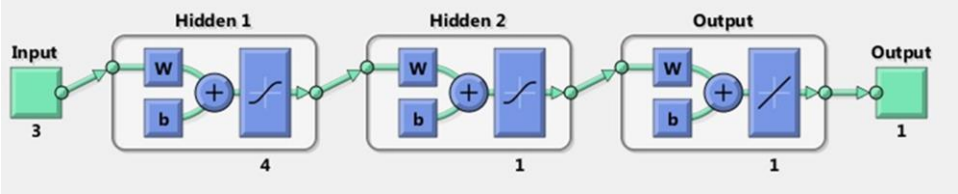

Figure 7. Structure of ANN model to predict the percentage of honey adulteration.

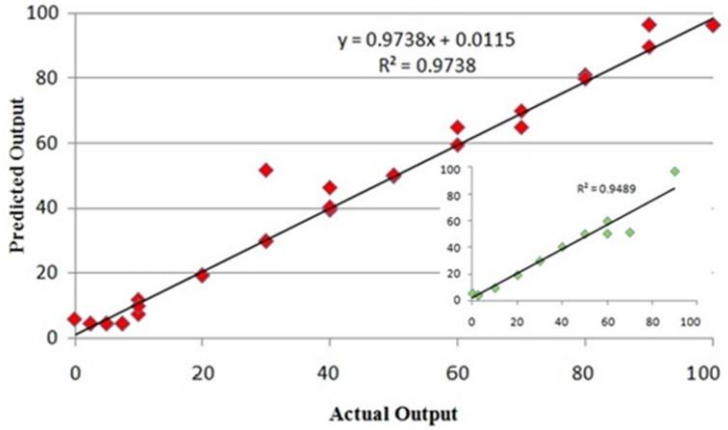

Figure 8. Correlation between actual data of honey adulteration (%) and ANN model predicted ones.

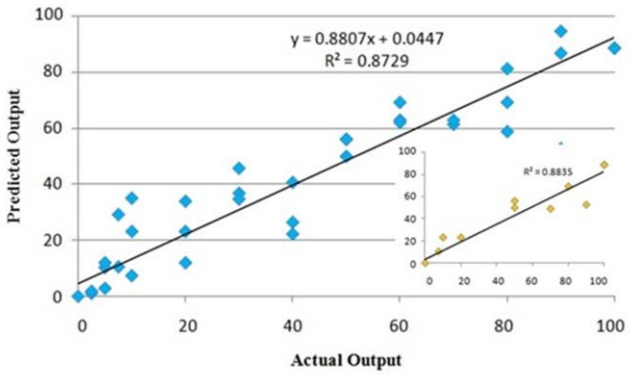

Figure 9. Correlation between actual data of honey adulteration (%) and predicted ones by the RSM model.

Table 3. Characteristics of the best ANN model to predict the percentage of honey adulteration.

Number of input	General network structure	Type of training function	Transfer functions
3	3-4-1-1	Levenberg-Marquardt	Tansig - Tansig -Purelin

Table 4. Performance parameters of the best ANN model to predict adulteration of honey.

	No. of data	MSE	MAE	SSE	R^2
Training	29	0.0024	0.0272	0.0703	0.9808
Test	12	0.0045	0.0388	0.0534	0.9489
All data	41	0.0030	0.0306	0.1237	0.9738

Table 5. Performance parameters of the RSM model for estimating honey adulteration.

	No of data	MSE	MAE	SSE	R^2
Training	29	0.0115	0.0824	0.3340	0.8940
Test	12	0.0224	0.1109	0.2683	0.8835
All data	41	0.0147	0.0907	0.6024	0.8729

adulteration was less than the other models used in this study.

Comparison Performance of ANFIS, ANN and RSM Models

The multi statistical criteria were used in order to evaluate the prediction ability of the developed models in this study, including ANFIS, ANN, and RSM. Comparison of some of these criteria and the residual error are seen in Figures 10 and 11. As can be seen clearly, in all data sets, the RSM model has higher MSE and deviation distribution than the other two models. Therefore, it is safe to say that the RSM power of predicting is less than the other two models. The evaluation criteria of the two models of ANFIS and ANN were very close to each other and made it difficult to choose the best model between them. Based on the desirability function graph (Figure 12), considering simultaneously all the errors and the coefficient of determination, the ANN model was the best model with desirability of 0.948. The least variation and deviation from the horizontal axis (Figure 12) for the ANN model is indicative of high desirability with the least residues in this model. Based on the lower error value in prediction, the ANN model had better performance than ANFIS model with desirability of 0.948 and 0.824, respectively.

CONCLUSIONS

This research proved the direct relation between the degree of honey adulteration and the average total amount of components (pollen and other natural insoluble solids) on the microscopic slide of honey deposition. Honey adulterations will reduce the amount of pollen and other solids in the honey deposition. The results showed that the microscopic image processing is able to identify different types of honey fraud with the least expertise and the simplest laboratory tools in the shortest time and cost. In this study, the determination coefficient of ANN model was 0.974 while the ANFIS and RSM models had values of 0.973 and 0.873, respectively. Also, the lowest deviation of the model output from the actual data (prediction

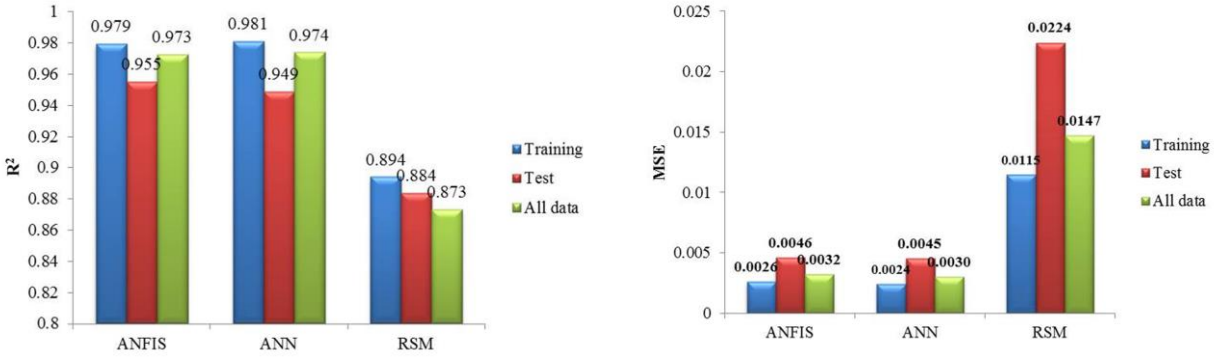

Figure 10. Performance parameters of the models for training, test, and all data to estimate the honey adulteration: (a) R^2, and (b) MSE values.

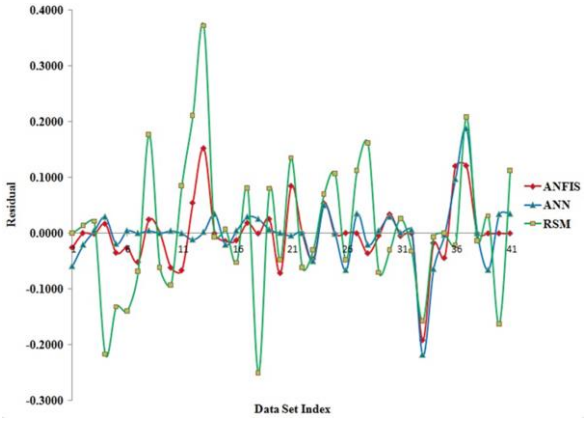

Figure 11. Comparison of distribution of residual values by the ANFIS, ANN and RSM models estimating honey adulteration.

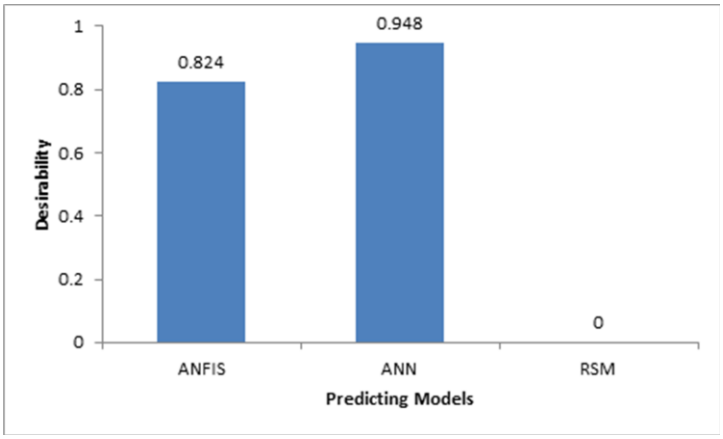

Figure 12. Desirability of all models for predicting honey adulteration.

error) was reported in the ANN model. The evaluation criteria of ANFIS and ANN were very close to each other and it was difficult to choose the best model between them. Therefore, by employing the desirability function and considering all the errors and the determination coefficient, the ANN model was the best model. The desirability of ANN and ANFIS model was 0.948 and 0.824, respectively. The results of this study showed that using new and simple tools and technologies, it is possible to detect fraud in honey with high accuracy and speed.

ACKNOWLEDGEMENTS

This study was not funded by any grant number, but the authors thank the Vice Chancellor for Research and Technology, Razi University, Iran. Also, all authors declare that they have no conflict of interest. This article does not contain any studies with human participants or animals performed by any of the authors.

REFERENCES

1. Standard, C. A. 2001. Revised Codex Standard for Honey. Revision 2. *24th Session of the Codex Alimentarius.*
2. Li, S., Shan, Y., Zhu, X., Zhang, X. and Ling, G. 2012. Detection of HoneyAdulteration by High Fructose Corn Syrup and Maltose Syrup Using Raman Spectroscopy. *J. Food Compost. Anal.*, **28**: 69-74.

3. Tosun, M. 2013. Detection of Aadulteration in Honey Samples Added Various Sugar Syrups with 13 C/12 C Isotope Ratio Analysis Method. *Food Chem.,* **138**: 1629-1632.
4. Agila, A. and Barringer, S. 2013. Effect of Adulteration versus Storage on Volatiles in Unifloral Honeys from Different Floral Sources and Locations. *J. Food Sci.,* **78**: 184-191.
5. Anthony, C. and Balasuriya, D. 2016. Electronic Honey Quality Analyser. *Engineer: Journal of the Institution of Engineers, Sri Lanka,* **49(3)**: 41-47. Cordella, C., Faucon, J. P., Cabrol-Bass, D. and Sbirrazzuoli, N. 2003. Application of DSC as a Tool for Honey Floral Species Characterization and Adulteration Detection. *JTAC,* **71**: 279-290. Du, B., Wu, L., Xue, X., Chen, L., Li, Y., Zhao, J. and Cao, W. 2015. Rapid Screening of Multiclass Syrup Adulterants in Honey by Ultrahigh-Performance Liquid Chromatography/Quadrupole Time of Flight Mass Spectrometry. *J. Agric. Food Chem.,* **63**: 6614-6623.
6. Zakaria, A., Shakaff, A. Y. M., Masnan, M. J., Ahmad, M. N., Adom, A. H., Jaafar, M. N., Ghani, S. A., Abdullah, A. H., Aziz, A. H. A. and Kamarudin, L. M. 2011. A Biomimetic Sensor for the Classification of Honeys of Different Floral Origin and the Detection of Adulteration. *Sensors,* **11**: 7799-7822.
7. Salvador, L., Guijarro, M., Rubio, D., Aucatoma, B., Guillén, T., Vargas Jentzsch, P., Ciobotă, V., Stolker, L., Ulic, S. and Vásquez, L. 2019. Exploratory Monitoring of the Quality and Authenticity of Commercial Honey in Ecuador. *Foods,* **8**: 105.
8. Du, C. J. and Sun, D. W. 2004. Recent Developments in the Applications of Image Processing Techniques for Food Quality Evaluation. *Trends Food Sci. Technol.,* **15**: 230-249.
9. Esteki, M., Farajmand, B., Kolahderazi, Y. and Simal-Gandara, J. 2017. Chromatographic fingerprinting with Multivariate Data Analysis for Detection and Quantification of Apricot Kernel in Almond Powder. *Food Anal. Methods,* **10**: 3312-3320.
10. Esteki, M., Simal-Gandara, J., Shahsavari, Z., Zandbaaf, S., Dashtaki, E. and Vander Heyden, Y. 2018. A Review on the Application of Chromatographic Methods, Coupled to Chemometrics, for Food Authentication. *Food Control.,* **93**: 165-182.
11. Esteki, M., Shahsavari, Z. and Simal-Gandara, J. 2018 Use of Spectroscopic Methods in Combination with Linear Discriminant Analysis for Authentication of Food Products. *Food Control.,* **91**:100-112.
12. Yang, M., Gao, Y., Liu, Y., Fan, X., Zhao, K. and Zhao, S. 2018. Broadband Dielectric Properties of Honey: Effect of Water Content. *J. Agr. Sci. Tech.,* **20**:685-693. Fahim Danesh, M. and Bahrami, M. E. 2015. Evaluation of Adulteration in Sesame Oil Using Differential Scanning Calorimetry. *Food Sci. Technol.,* **13**:81-89.
13. Khorsandmanesh, S., Gharachorloo, M., Bahmaie, M., Moghaddam, A. Z. and Azizinezhad, R. 2020. Sterol and Squalene as Indicators of Adulteration of Milk Fat with Palm Oil and Its Fractions. *J. Agr. Sci. Tech*., **22(5)**: 1257-1266.
14. Shafiee, S., Polder, G., Minaei, S., Moghadam-Charkari, N., Van Ruth, S. and Kuś, P. M. 2016. Detection of Honey Adulteration using Hyperspectral Imaging. *IFAC-Papers OnLine,* **49**: 311-314.
15. Cseke, I., Fazekas, Z. and Holka, T. 1993. Honey Qualification: An Application of the ARGUS Image Processing System. *Microprocess. Microsyst.,* **17**: 219-222.
16. Kerkvliet, J., Shrestha, M., Tuladhar, K. and Manandhar, H. 1995. Microscopic Detection of Adulteration of Honey with Cane Sugar and Cane Sugar Products. *Apidologie,* **26**: 131-139.
17. Anjos, O., Iglesias, C., Peres, F., Martínez, J., García, Á. and Taboada, J. 2015. Neural Networks Applied to Discriminate Botanical Origin of Honeys. *Food Chem.,* **175**: 128-136.
18. D'Ávila, V., Aguiar-Menezes, E., Gonçalves-Esteves, V., Mendonça, C., Pereira, R. and Santos, T. 2016. Morphological Characterization of Pollens from Three *Apiaceae* Species and Their Ingestion by Twelve-Spotted Lady Beetle (Coleoptera: Coccinellidae). *Braz. J. Biol.,* **76**: 796-803.
19. Asadi, M. 2006. *Beet-Sugar Handbook*. John Wiley & Sons.
20. Bidin, N., Zainuddin, N. H., Islam, S., Abdullah, M., Marsin, F. M. and Yasin, M. 2016. Sugar Detection in Adulterated Honey

via Fiber Optic Displacement Sensor for Food Industrial Applications. *IEEE Sens. J.*, **16**: 299-305.
21. Gonzalez, R. C. and Woods, R. E. 2002. *Digital Image Processing Prentice Hall.* Upper Saddle River, NJ.
22. Mostafaei, M. 2018. ANFIS Models for Prediction of Biodiesel Fuels Cetane Number Using Desirability Function. *Fuel*, **216**: 665-672.
23. Myers, R. H., Montgomery, D. C. and Anderson-Cook, C. M. 2016. Response Surface Methodology: Process and Product Optimization Using Designed Experiments. John Wiley & Sons.
24. Ou, W. -J., Meng, Y. -Y., Zhang, X. -Y. and Kong, M. 2011Application of UV-Visible Absorption Spectroscopy and Principal Components-Back Propagation Artificial Neural Network to Identification of Authentic and Adulterated Honeys. *Chinese J. Anal. Chem.*, **39**: 1104-1108.
25. Irudayaraj, J., Xu, R. and Tewari, J. 2003. Rapid Determination of Invert Cane Sugar Adulteration in Honey Using FTIR Spectroscopy and Multivariate Analysis. *J. Food Sci.*, **68**: 2040-2045.
26. Chen, Q., Qi, S., Li, H., Han X., Ouyang, Q. and Zhao, J. 2014. Determination of Rice Syrup Adulterant Concentration in Honey Using Three-Dimensional Fluorescence Spectra and Multivariate Calibrations. *Spectrochim. Acta A Mol. Biomol. Spectrosc.*, **131**: 177-182.
27. Ouyang, Q. 2013. Identification of Adulterated Honey Based on Three-Dimensional Fluorescence Spectra Technology. *Spectroscopy and Spectral Analysis*, **33**: 1626-1630.

مدل سازی تقلب در عسل بر اساس پردازش تصاویر میکروسکوپی به کمک روش‌های هوش مصنوعی

م. پیر مرادی، م. مصطفایی، ل. ندرلو، و ح. جوادی کیا

چکیده

هدف از این مطالعه تعیین اصالت عسل با پردازش تصاویر میکروسکوپی و بدست آوردن الگوریتمی برای طبقه‌بندی تقلب‌های مختلف عسل است. در این مطالعه از ساکارز، فروکتوز و محلول فروکتوز – گلوکز با نسبت 0.9 برای ایجاد تقلب در عسل استفاده شد. سطح تقلب عسل براساس درصد وزنی 2.5 ، 5 ، 7.5 ، 10 ، 20 ، 30 ، 40 ، 50 ، 60 ، 70 ، 80 ، 90 و 100 با هم زدن ایجاد شد. نمونه های مختلف زیر میکروسکوپ تصویربرداری شد. هر تصویر در 33 فضای رنگی تک رنگ پردازش و 15 پارامتر از آن استخراج شد. با استفاده از تجزیه و تحلیل حساسیت سه پارامتر اصلی و موثر از فضاهای رنگی مختلف برای مدل سازی تقلب عسل توسط سیستم استنباط عصبی فازی تطبیقی، شبکه عصبی مصنوعی و روش سطح پاسخ انتخاب شد. برای ارزیابی عملکرد مدل‌ها از معیارهای مختلفی مانند ضریب تبیین ، میانگین مربعات خطا، مجموع توان‌های دوم باقیمانده‌ها و میانگین مطلق خطا استفاده شد. نتایج نشان داد که ضریب تبیین و میانگین مربعات خطا در مدل شبکه عصبی مصنوعی به ترتیب 0/974 و 0/0024 بوده است. این بهترین مدل با عملکرد مطلوب 0.948 و خطای پیش بینی کمتر

بود. در نهایت، با استفاده از تابع مطلوبیت، به دلیل مقادیر خطای پیش بینی کمتر و مطلوبیت 0.948، مدل شبکه عصبی مصنوعی به عنوان بهترین مدل انتخاب شد.